Effects of particle size and gasification atmosphere on the changes in char structure during the gasification of mallee biomass

Shuai Wang, Liping Wu, Xun Hu, Lei Zhang, Tingting Li and Chun-Zhu Li*

Fuels and Energy Technology Institute, Curtin University of Technology, GPO Box U1987, Perth, WA 6845, Australia

Submitted to

Energy & Fuels

For consideration of publication

Apr 2018

*Corresponding author: chun-zhu.li@curtin.edu.au; telephone: +61 8 9266 1131; facsimile: +61 8 9266 1138

Abstract

The purpose of this study is to investigate the evolution of char structure during the gasification of mallee biomass in different particle size ranges (up to 5.6 mm) in two atmospheres (15% H_2O balanced with Ar and pure CO_2) in a fluidised-bed reactor. FT-Raman spectroscopy was used to characterise the char structure. The first-order Raman spectra in the range between 800 and 1800 cm^{-1} and the second-order Raman spectra in the range between 2200 and 3300 cm^{-1} were deconvoluted to understand the detailed structural features of char. Our results show that the differences in the intra-particle heat and mass transfer between small and big particle sizes during pyrolysis are largely responsible for the difference in char yield during gasification, and the intra-particle gas diffusion is not a rate-limited step during the subsequent gasification of char for the conditions used in this study. As revealed by the Raman spectroscopy, there are no significant changes in the overall Raman-active oxygen species and aromatic ring systems among different biomass particle sizes during gasification. The differences in the crossing-linking density of char as indicated by the 2S band in the second-order Raman spectra between gasification in steam and CO_2 atmosphere again demonstrate that the char-H_2O and char-CO_2 follow different reaction pathways.

Keywords: Biomass particle size; Char gasification; FT-Raman spectroscopy; Char structure

1. Introduction

With the depletion of fossil fuel resources and the rising concerns about global warming, biomass as a renewable energy source has received a great deal of interests in recent years due to its abundance and low environmental impacts [1-2]. Biomass gasification is an effective technology to convert solid biomass into a gaseous fuel for further use [3-6]. However, biomass gasification must overcome some practical problems before its widespread commercial implementation. One of the problems is the size range of the feedstock [7-11]. It is impossible to obtain a specified narrow biomass particle size range as the feedstock for a practical gasifier/pyroliser because the size reduction of biomass is very labour-intensive and time-consuming, making it commercially unattractive [12]. Therefore, the feedstock for a commercial gasifier necessarily consists of particles with a wide range of sizes [12].

Gasification rate is a major consideration in the design and operation of a practical gasifier because it would determine the overall efficiency and economic feasibility of the gasifier [12-17]. The evolution of char structure is an important factor that can influence the gasification behaviour [1,2]. Therefore, understanding the influence of biomass particle size on the ultimate char yield and the structural feature of char during gasification is significantly important for the development of gasification technologies.

Conceptually, the gasification process consists of two consecutive steps although a clear distinction between the two steps may not always be possible [2]. The first step is the biomass devolatilisation, leaving behind a carbon-enriched solid char. Because of the high contents of oxygen and aliphatic moieties of biomass, large

amounts of volatiles or volatile precursors would be formed in this step [2,18,19]. These newly formed volatile precursors could participate in the deposition reaction in char matrix [20-22]. Because there are differences in the heating transfer resistance as well as the intra-particle mass transfer resistance between small and large particles, the deposition reaction would be more severe for large particles than for small ones [21-26]. The second step is the char gasification and volatile reforming through their reactions with gasifying agents. The difference in the intra-particle diffusion of the gasifying agent between small and large particles might also have an effect on the gasification rate and the overall char structure.

Some studies have been carried out to investigate the effects of biomass particle size on the evolution of char structure as revealed by the Raman spectroscopy [20-22]. Asadullah and co-workers reported that biomass particle size would greatly influence the char yield during pyrolysis [20,21]. Zhang and co-workers [22] reported that, based on the negligibly small influence of the biomass particle size on the change in char structure during gasification in steam atmosphere, the gasification might take place uniformly throughout the whole particles. However, these researches did not provide the direct evidence that whether the size of char produced from the biomass devolatilisation would affect the ultimate char yield and char structures during the subsequent gasification. In other words, the effect of intra-particle diffusion of the gasifying agent between small and large particles during gasification has not been directly investigated.

Char-steam gasification and char-CO_2 gasification are both fundamentally important reactions. A better understanding the mechanisms of the char-H_2O reaction and char-CO_2 reaction is necessary for the development of gasification technologies [27]. One question raised is: does biomass particle size affect the

evolution of char structure during the gasification in steam atmosphere and CO_2 atmosphere? Therefore, investigation on the gasification behaviour of different biomass particle sizes in steam atmosphere and CO_2 atmosphere can provide another aspect to understand the char-H_2O and char-CO_2 reaction mechanism. In addition, second-order Raman spectroscopy can also be used to characterise the char structure [28]. Complementary or additional information about the structural feature of char can be found through the analysis of the second-order Raman spectra.

The objective of this research is to comprehensively investigate the influence of biomass particle size and gasification atmosphere on the ultimate char yield as well as the evolution of char structure, especially in the aspect of the intra-particle diffusion of the gasifying agent during the gasification of char with different particle sizes. As discussed above, the devolatilisation and the gasification might be both influenced by the biomass particle size. In order to clarify these two possibilities, two series of experiments were carried out in this study. The first series was the gasification of biomass with different particle sizes at the temperatures from 700 to 900 ˚C in two atmospheres: 15 % H_2O balance with Ar and pure CO_2. The other series was the char gasification experiments, which would separate the biomass devolatilisation step and char gasification step during gasification. The collected char samples were analysed with a FT-Raman spectrometer both in the first-order Raman spectral region and second-order Raman spectral region to obtain information about the chemical structural features of the chars.

2. Experimental

2.1 Sample preparation

Australia mallee wood was used as the feedstock in this study. It has a proximate analysis of 0.9 wt% ash yield and 81.6 wt% volatiles yield together with an ultimate composition of 48.2 wt% C, 6.1 wt% H, 0.2 wt% N and 45.5 wt% O (dry and ash-free basis) [20-22]. The preparation of the wood sample can be found elsewhere [20-22]. Briefly, the mallee wood was firstly debarked and crushed into chips using a cutting mill and then eight wood samples with different particle sizes were obtained by sieving. The particle sizes of the eight wood samples are as follow: 0.18-0.40, 0.40-0.80, 0.80-1.00, 1.00-2.00, 2.00-3.35, 3.35-4.00, 4.00-4.75, 4.75-5.60 mm. All biomass samples were stored in a freezer to avoid any biological degradation and the samples were dried in oven overnight at 105 ˚C before the experiment.

2.2 Experimental procedure

Biomass gasification experiments were carried out in a fluidised-bed quartz reactor [20] with fast heating rate (1000 K/s). The schematic diagram of the fluidized-bed reactor is shown in Figure 1. Briefly, the reactor was heated up to the target temperature (700, 800 or 900 ˚C) with an external furnace with the introduction of the gasifying agent (15 % H_2O balance with Ar or pure CO_2) into the reactor. When all the parameters were stabilised, about 2 g biomass (weighed accurately) was fed into the reactor within 4 minutes. The reactor was lifted out of the furnace immediately when the feeding was completed and was cooled down naturally with argon flowing inside the reactor instead of the gasifying agent.

Char gasification experiments were carried out in the same reactor, which would separate the pyrolysis process and gasification process during the biomass gasification. The first step was the char preparation. Mallee wood with the particle size between 4.75-5.60 mm was pyrolysed at 900 ˚C under fast heating rates by feeding the biomass into the pre-heated reactor continuously. When the feeding was completed, the reactor was held for 30 minutes at 900 ˚C. The collected char sample was grounded and sieved to the following five particle sizes: 0.18-0.50, 0.50-1.00, 1.00-2.00, 2.00-3.35, 3.35-4.75 mm. The next step was to use these char samples as the feedstock to do the char gasification experiments. About 0.2 g char (weighed accurately) was pre-loaded into the fluidised-bed reactor and the reactor was heated up to 900 ˚C in argon atmosphere. When the desired temperature was reached, the gasifying agent was introduced into the reactor for 10 minutes. The experiment was also terminated by lifting the reactor out of the furnace.

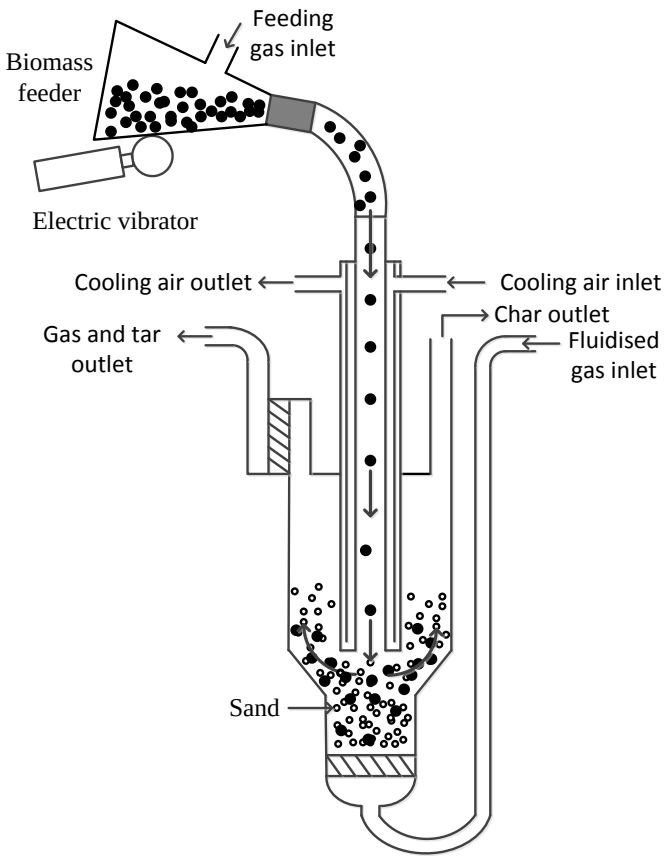

Fig. 1. A schematic diagram of the fluidized-bed reactor for the gasification of biomass under the fast heating rate conditions. (Redraw based on Ref [20] with some modifications)

2.3 Char characterisation

A Perkin-Elmer GX FT-IR/Raman spectrometer with an excitation laser of 1064 nm was used for the characterisation of char structure following the procedure has been established previously [29]. Briefly, the char sample was mixed and ground with spectroscopic grade KBr, which acted as a heat-dissipating medium to prevent char sample from being heated up by the laser. A concentration of 0.5 wt% char in the char-KBr mixture was selected, which achieved the plateau in the total Raman area both for the first-order Raman region (800-1800 cm^{-1}) [20-22] and the second-order Raman region (2000-3300 cm^{-1}). Each of the acquired Raman spectra was further deconvoluted in order to understand the specific chemical structure of the

char. The first-order Raman spectra were deconvolution into 10 Gaussian bands and the second-order Raman spectra were deconvolution into 8 Gaussian bands to obtain the detailed structural features of char. The detail assignment of these bands can be found elsewhere [28,29]. One modification has been made on the deconvolution method of the second-order Raman spectra because of the presence of an additional peak at around 2950 cm^{-1} for the chars from low temperature gasification (700 ˚C). This band was originated from the overtone of V_L band in the first-order [28,29], thus named as $2V_L$, representing amorphous carbon structures. A typical example of the spectral deconvolution of the first and second-order Raman spectra of chars is shown in Figure 2. The relative standard deviation of the first-order Raman analysis was within 5%, and the relative standard deviation of the second-order Raman analysis was within 10%.

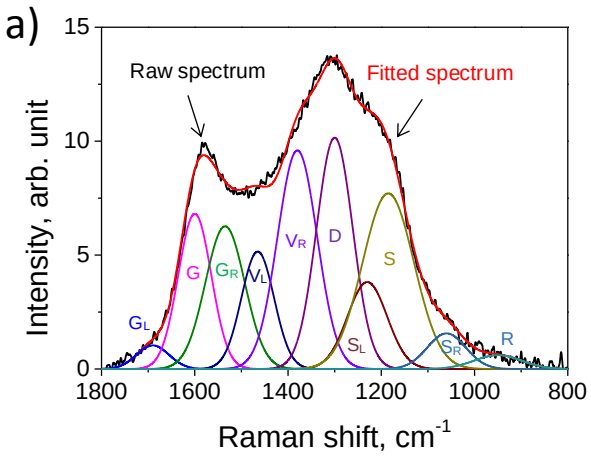

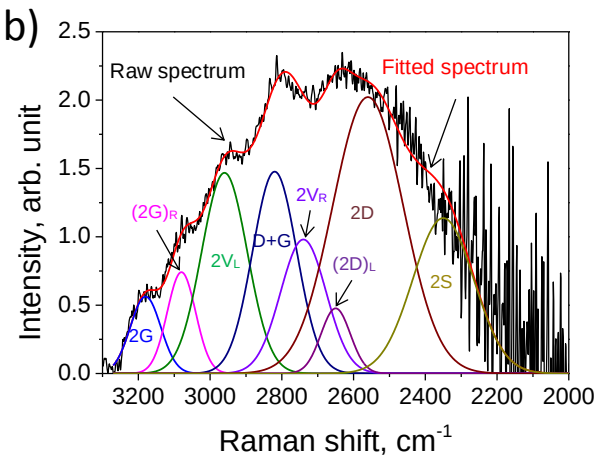

Fig. 2. Spectral deconvolution of a Raman spectrum in (a) first-order region and (b) second-order region of the chars from gasification in 15% H_2O-Ar at 700 ˚C.

3. Results and discussion

3.1 Char yield

Figure 3 shows the char yield as a function of biomass particle size as well as temperature. As expected, high temperature would enhance the devolatilisation and gasification of char [20-22]. Therefore, for a given particles size, the char yield decreased with increasing temperature. In addition, at a specified temperature, the char yield increased with increasing particle size both for the gasification in steam atmosphere and CO_2 atmosphere. Two reasons could be responsible for this trend. One is the differences between small and large particles in transporting the volatiles especially the tarry compounds out of the pyrolysing particles [21]. The mallee wood sample used in this study has a volatile yield of 81.6 wt% [21-22], and large amounts of volatiles would be released during pyrolysis. The residence time of the volatiles would be much longer in a large particle than in a small one. In addition, a high heating rate for a small particle could cause the quick formation of volatiles and thus result in a rapid pressure increase in the particle, which could also lead to a short

residence time of volatiles in char. In addition, more volatiles would recondense or reabsorb on the internal surface of the char from a large particle than that from a small one, resulting in increases in the char yield. The other reason for the increasing char yield with increasing particle size in Figure 3 could be the difference in the intra-particle diffusion of the gasifying agent between small and big particles, which could potentially result in different gasification rates for different particle sizes.

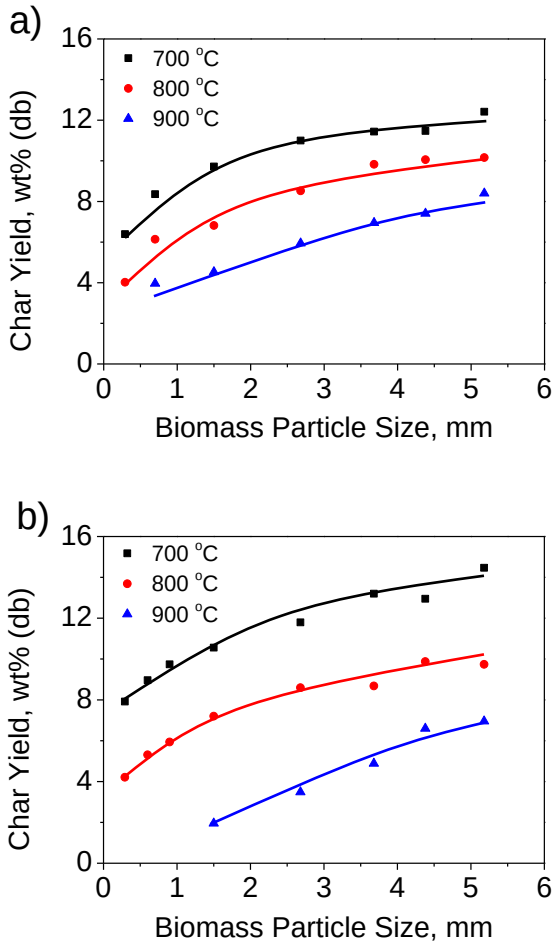

Fig. 3. Char yields as a function of average biomass particle size during the gasification of mallee wood at 700, 800 and 900 ˚C in (a) 15% H_2O balanced with Ar; (b) pure CO_2.

Further experiments were then carried out on the gasification of char with different particle sizes to understand the relative importance of above-mentioned two possible reasons. Char samples of different particle sizes were prepared by crushing the same large char sample to ensure the identical structural feature. Figure 4 illustrates

the effects of char particle size on the conversion of char in steam atmosphere and CO_2 atmosphere. The conversion of char was almost the same regardless of particle size in the cases of gasification in steam atmosphere and in CO_2 atmosphere, which indicated that there was plenty of time for the gasifying agent to penetrate into the char particles before the reaction took place. In other words, the intra-particle gas diffusion was not the rate-limiting step during gasification for the conditions used in this study. Therefore, the changes in the char yield with biomass particle size (Figure 3) were mainly due to the difference in the residence time of volatiles in small and big particles. A long residence time would tend to enhance the formation of additional coke from the volatiles within a pyrolysing biomass particle.

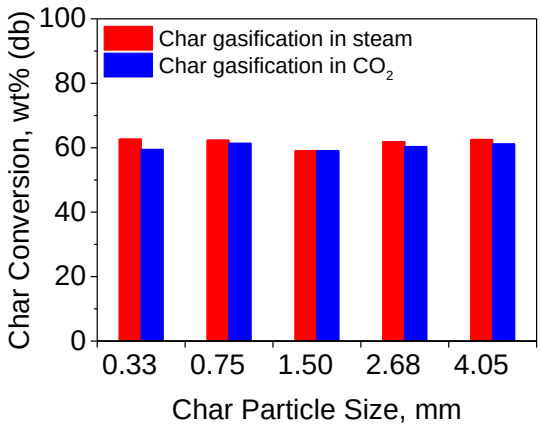

Fig. 4. Char conversion as a function of the average char particle size during the gasification at 900 ˚C in 15% H_2O balanced with Ar and in pure CO_2. Char samples of different particle sizes were prepared by crushing the same large char sample.

3.2 Char structure

3.2.1 Oxygenation of the char

The total peak area of a first-order Raman spectrum was taken as the total intensity in the range between 800 and 1800 cm^{-1}. Both Raman scattering ability and light absorption ability of char could affect the observed Raman intensity [29]. The

electron rich structures such as the O-containing structure in char can exert a resonance effect between oxygen and aromatic ring to which oxygen is connected, which could enhance the total Raman intensity. In addition, the light absorptivity of char would be enhanced by the growth of aromatic ring systems, resulting in declines in the observed total Raman intensity [29]. Figure 5 exhibits the influences of biomass particle size on the total band area of the first-order Raman at different gasification temperatures. For the biomass gasification both in steam atmosphere and CO_2 atmosphere, the total Raman intensity decreased with increasing gasification temperature, especially from 700 to 800 ˚C. This decrease implies that the release of O-containing structure through thermal cracking and the growth of the aromatic ring system of char during gasification [20-22,27]. These changes would be intensified with increasing temperature. In addition, there should be much more recondensed volatiles in the char matrix of big particles than that of small particles [21,22]. However, the total intensity of the first-order Raman was not affected by biomass particle size. Therefore, this result indicated that the recondensed volatiles did not result in significant changes in the overall Raman-active oxygen species of char during gasification. This observation is in agreement with our previous study [22].

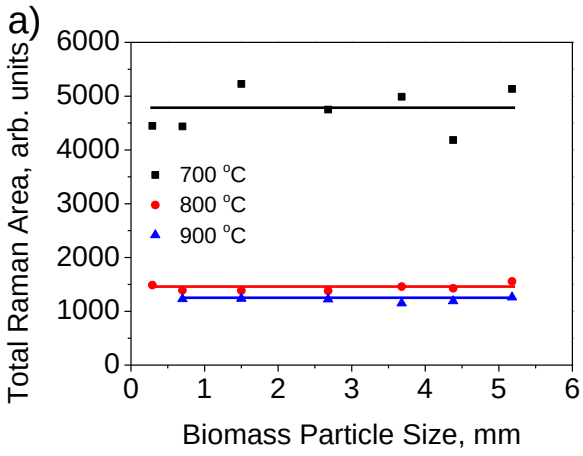

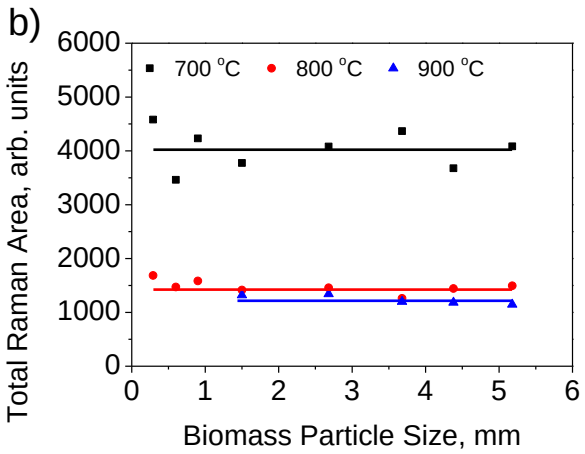

Fig. 5. Total first-order Raman area as a function of average biomass particle size during the gasification of mallee wood at 700, 800 and 900 ˚C in (a) 15% H_2O balanced with Ar; (b) pure CO_2.

Figure 6 illustrates the total intensity of the first-order Raman of char prepared from pyrolysis and then experienced the gasification in steam atmosphere and CO_2 atmosphere with different char particle sizes. The total Raman intensity of char produced from pyrolysis was significantly lower than that after experiencing the gasification, indicating that some oxygen derived from H_2O and CO_2 would possibly form oxygen complexes on char matrix [27,30,31]. In addition, for different char particle sizes, the total Raman intensity of char was almost the same, both for the gasification in steam atmosphere and CO_2 atmosphere. It means that the gasification may take place uniformly throughout the whole particles [22], regardless of the particle size. Furthermore, comparing the total Raman intensity of char from gasification in steam with that in CO_2, the total intensity of char prepared from the gasification in steam was much higher than that in CO_2, indicating that more Raman-active O-containing species connected with aromatic ring system in steam than that in CO_2 [27]. Moreover, comparing the total Raman intensity of char produced from the biomass gasification (Figure 5) with that from the char gasification (Figure 6) under 900 ˚C, it can be seen that for the gasification in steam, the total Raman

intensity of char produced from char gasification with 10 minutes holding time was higher than that produced form biomass gasification with 4 minutes feeding time, which means that the char structures became increasingly oxygenated with the progress of gasification in steam. However, for the gasification in CO_2, the total Raman intensity was almost the same, regardless of the reaction time. This result indicated that the oxygen complexes formed on char during the gasification in steam atmosphere and CO_2 atmosphere were different. The oxygen spices formed in steam atmosphere should be more Raman-active than that formed in CO_2 atmosphere. Therefore, the different gasification behaviour in terms of the total Raman intensity between the gasification in steam atmosphere and CO_2 atmosphere indicated that the char-H_2O and char-CO_2 reactions followed different reaction pathway [27].

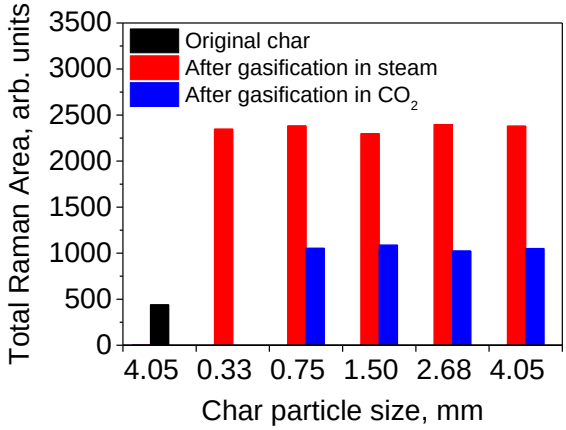

Fig. 6. Total first-order Raman area as a function of average char particle size during the pyrolysis of mallee wood at 900 ˚C in Ar, pyrolysis and subsequent gasification of char at 900 ˚C in 15% H_2O balanced with Ar, pyrolysis and subsequent gasification of char at 900 ˚C in pure CO_2.

3.2.2 Change in the aromatic ring systems in char

Based on the bands assignment of the first-order Raman spectrum [29], the I_D mainly represents the large aromatic ring systems with no less than 6 fused rings, while the $I_{(Gr+Vl+Vr)}$ mainly represents the small aromatic ring systems with less than 6

fused rings. Therefore, the band area ratio $I_D/I_{(Gr+Vl+Vr)}$ can be used as an indirect indication of the relative ratio of large to small aromatic ring systems in char [29].

As is shown in Figure 7, for the gasification both in steam atmosphere and CO_2 atmosphere, a higher temperature tended to result in a higher $I_D/I_{(Gr+Vl+Vr)}$ ratio. High temperature means fierce thermal cracking and gasification reaction which would enhance the selective removal of small aromatic systems and the conversion of small aromatic systems to large ones in char [27,30,31]. Furthermore, for a given temperature, this ratio was constant, regardless of particle sizes, which confirmed that the coke or soot formed from the recondensed volatiles had structural features (as observed with FT-Raman spectroscopy) similar to those in char during gasification [22].

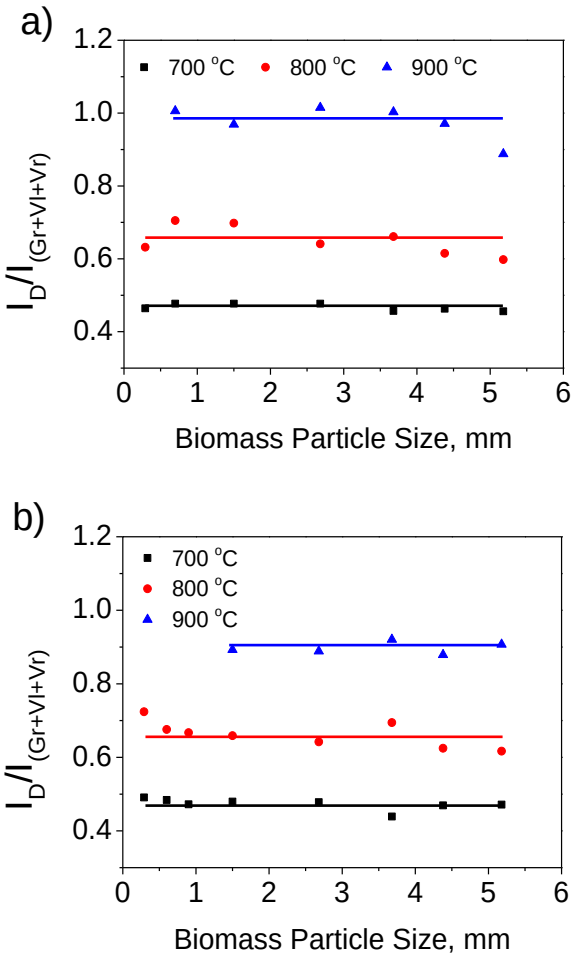

Fig. 7. Raman band area ratios D/Gr+Vl+Vr as a function of average biomass particle size during the gasification of mallee wood at 700, 800 and 900 ˚C in (a) 15% H_2O balanced with Ar; (b) pure CO_2.

Figure 8 illustrates the band area ratios $I_D/I_{(Gr+Vl+Vr)}$ of chars prepared from pyrolysis and chars that also experienced the gasification in steam atmosphere and CO_2 atmosphere. The band ratios $I_D/I_{(Gr+Vl+Vr)}$ of chars produced from pyrolysis was lower than that after gasification, indicating that the gasification process would enhance the selective removal of small aromatic systems and the conversion of small aromatic systems to large ones in char [27,30,31]. In addition, both for the gasification in steam and CO_2, the band ratios $I_D/I_{(Gr+Vl+Vr)}$ of chars were almost constant with the particle size. These results were consistent with the analysis results of the total Raman intensity of chars of different particle sizes during the char gasification experiments, confirming that the gasification took place uniformly throughout the whole particles [22].

Furthermore, the band ratios $I_D/I_{(Gr+Vl+Vr)}$ of chars produced from gasification in steam were much higher than those in CO_2. This was mainly due to the H radicals generated from H_2O during gasification would penetrate into the char matrix and induce the aromatic ring condensation reactions [27]. Therefore, the conversion of small aromatic systems to large aromatic systems was more pronounced in steam atmosphere than that in CO_2 atmosphere, resulting in the higher band area ratio. Moreover, making the comparison of the band ratios $I_D/I_{(Gr+Vl+Vr)}$ of chars between that from the biomass gasification with 4 minutes feeding time (Figure 7) and that from the char gasification with 10 minutes holding time (Figure 8) at 900 ˚C, both for the gasification in steam and CO_2, the small aromatic rings were more preferred to be consumed by the gasifying agent than the large aromatic rings with the progress of gasification, resulting in increases in the band ratio $I_D/I_{(Gr+Vl+Vr)}$.

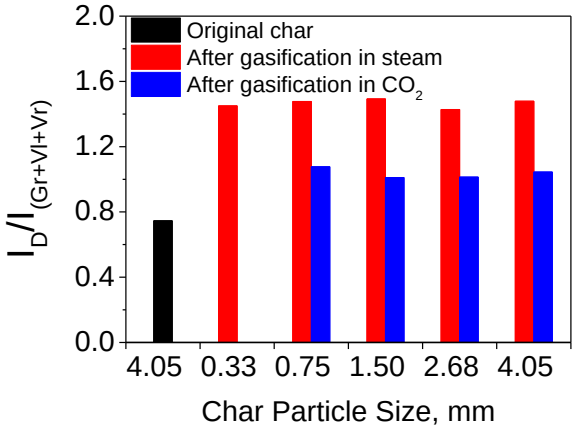

Fig. 8. Raman band area ratios D/Gr+Vl+Vr as a function of average char particle size during the pyrolysis of mallee wood at 900 ˚C in Ar, pyrolysis and subsequent gasification of char at 900 ˚C in 15% H_2O balanced with Ar, pyrolysis and subsequent gasification of char at 900 ˚C in pure CO_2.

3.2.3 Change in the crossing-linking structure in char

Amorphous carbon such as chars produced from gasification should contain lots of sp^3-rich structures [28,29]. Based on the band assignment of the Raman spectrum, the presence of the alkyl-aryl C-C structures, substitutional groups (other than O-containing ones) as well as the crossing-linking density in char can be indicated by the intensity of S band [29]. Meanwhile, the intensity of the 2S band in the second-order can also be used as an indication of the structural feature of char [28]. Although some studies indicated that the bandwidth as well as the intensity of 2S band decreased with the increasing crystallinity of the carbon-based materials [32-34], the structural feature of the low temperature (below 900 ˚C) gasified char was much different compared with that high temperature (above 1200 ˚C) treated carbon-based material. Therefore, in this study, the intensity of 2S band was also used to indicate the crossing-linking density of char [28]. The most important additional finding in the analysis of the second-order spectrum was the changes in the intensity of the 2S band during gasification while the intensity of S band in the first-order Raman did not show clear change during gasification.

Figure 9 shows the intensity ratios I_{2S}/I_{Total} as a function of the biomass particle sizes and gasification temperature. Both for the gasification in steam atmosphere and CO_2 atmosphere, the ratios I_{2S}/I_{Total} were almost the same for chars produced at 800 and 900 ˚C and were significantly lower than that at 700 ˚C. These results indicated the loss of the crossing-linking density in char with increasing gasification temperature, especially when the temperature was reached 800 ˚C. Also this ratio did not change with the biomass particle size. The data show some fluctuation when the gasification temperature reached 800 ˚C. This was mainly because that the total Raman intensity of the second-order was very weak for the chars produced from gasification in steam atmosphere and CO_2 atmosphere at 800 and 900 ˚C, so the deconvolution of the second-order spectrum would suffer from low signal-to-noise ratios, resulting in increased scatters. Therefore, the error bars have been given for 800 and 900 ˚C in Figure 9.

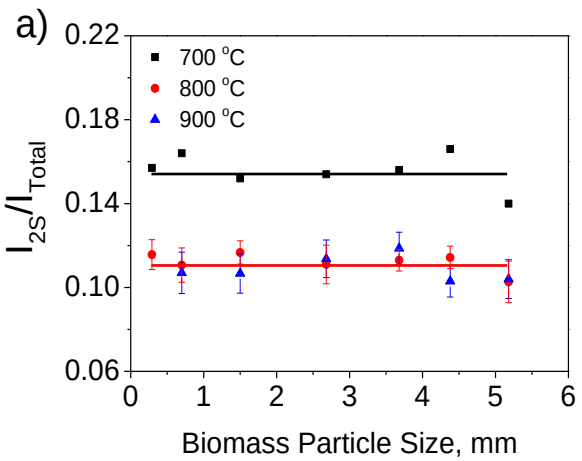

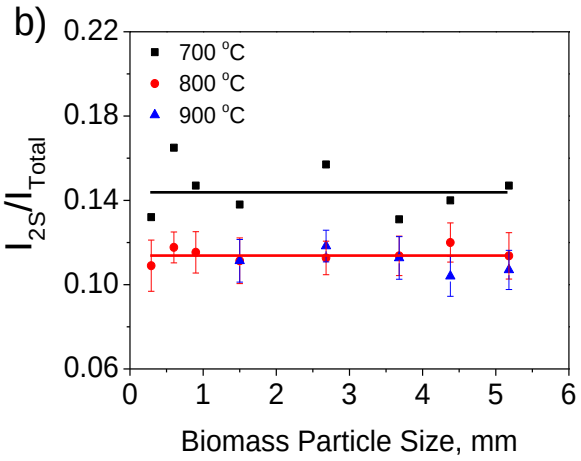

Fig. 9. Raman band area ratios 2S/Total as a function of average biomass particle size during the gasification of mallee wood at 700, 800 and 900 ˚C in (a) 15% H_2O balanced with Ar; (b) pure CO_2.

Figure 10 illustrates the effect of char particle on the change in the band area ratio I_{2S}/I_{Total} during gasification in steam atmosphere and CO_2 atmosphere at 900 ˚C (such ratio of char from pyrolysis at 900 ˚C is not displayed here due to the low intensity of the second-order Raman making it very difficult to get a reliable deconvolution result). It can be seen that the band area ratio I_{2S}/I_{Total} of char from the gasification in steam tended to be lower than that in CO_2. This could be also explained by the presence of H radicals during gasification in steam atmosphere, which would greatly activate the aromatic rings of char for the drastic growth of large aromatic ring systems, resulting in the loss of the crossing-linking density in char compared with that in CO_2 atmosphere.

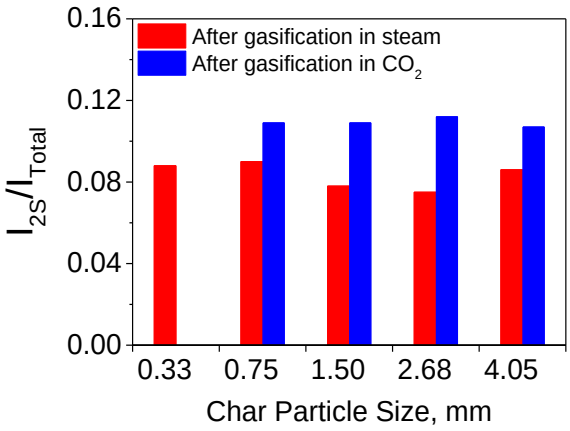

Fig. 10. Raman band area ratios 2S/Total as a function of average char particle size during the pyrolysis of mallee wood in Ar and subsequent gasification of char in 15% H_2O balanced with Ar at 900 ˚C, pyrolysis of mallee wood in Ar and subsequent gasification of char in pure CO_2 at 900 ˚C.

4. Conclusions

The influence of biomass particle size and gasification atmosphere in the char yield and evolution of char structure was investigated. The increased char yield with increasing biomass particle size during the gasification of biomass was mainly due to the increased heat and intra-particle mass transfer resistance in transporting the volatiles out of particles during the devolatilisation step. The subsequent gasification was not rate-limited by intra-particle diffusion of the gasifying agent under the present experimental conditions. The structural features of char changed drastically during the subsequent gasification. The biomass particle size had minimal effect on char structure, both for the gasification in steam atmosphere and CO_2 atmosphere, which means that the recondensed volatiles did not result in significant changes in the overall char structure during gasification and the gasification might take place uniformly throughout the char particle, regardless of the particle size under the present experimental conditions. The differences in char structure as revealed by

Raman spectroscopy confirmed that the char-H_2O and char-CO_2 reaction follow different reaction pathway.

Acknowledgements

This project received funding from the Australian Government through ARENA's Emerging Renewables Programs. The authors also greatly acknowledge the financial supports of this research from the Australian Research Council (DP110105514), Australia-China Science and Research Found.

References

[1] McKendry, P. Energy Production from Biomass (part 1): Overview of Biomass. Bioresour. Technol. **2002**, 83, 37-46.

[2] Li, C.-Z. Importance of Volatile-char Interactions during the Pyrolysis and Gasification of Low-rank Fuels – A Review. Fuel **2013**, 112, 609-623.

[3] Li, C.-Z. Special issue-gasification: A Route to Clean Energy. Process Saf. Environ. Prot. **2006**, 84, 407-408.

[4] Lasa, H.; Salaices, E.; Mazumder, J.; Lucky, R. Catalytic Steam Gasification of Biomass: Catalysts, Thermodynamics and Kinetics. Chem. Rev. **2011**, 111, 5404-5433.

[5] Huber, G.W.; Iborra, S.; Corma, A. Synthesis of Transportation Fuels from Biomass: Chemistry, Catalysts, and Engineering. Chem. Rev. **2006**, 106, 4044-4098.

[6] Navarro, R.M.; Pena, M.A.; Fierro, J.L.G. Hydrogen Production Reactions from Carbon Feedstocks: Fossil Fuels and Biomass. Chem. Rev. **2007**, 107, 3952-3991.

[7] Hernandez, J.J.; Aranda-Almansa, G.; Bula, A. Gasification of Biomass Wastes in an Entrained Flow Gasifier: Effect of the Particle Size and the Residence Time. Fuel Process. Technol. **2010**, 91, 681-692.

[8] Yin, R.; Liu, R.; Wu, J.; Wu, X.; Sun, C.; Wu, C. Influence of Particle Size on Performance of a Pilot-scale Fixed-bed Gasification System. Bioresour. Technol. **2012**, 119, 15-21.

[9] Gaston, K.R.; Jarvis, M.W.; Pepiot, P.; Smith, K.M.; Frederick, W.J.; Nimlos, M.R. Biomass Pyrolysis and Gasification of Varying Particle Sizes in a Fluidized-bed Reactor. Energy Fuels **2011**, 25, 3747-3757.

[10] Luo, S.; Xiao, B.; Guo, X.; Hu, Z.; Liu, S.; He, M. Hydrogen-rich Gas from Catalytic Steam Gasification of Biomass in a Fixed Bed Reactor: Influence of Particle Size on Gasification Performance. Int. J. Hydrogen Energy **2009**, 34, 1260-1264.

[11] McKendry, P. Energy Production from Biomass (part 3): Gasification Technologies. Bioresour. Technol. **2002**, 83, 55-63.

[12] Tiangco, V.M.; Jenkins, B.M.; Goss, J.R. Optimum Specific Gasification Rate for Static Bed Rice Hull Gasifiers. Biomass Bioenergy **1996**, 11, 51-62.

[13] Jin, G. Multiscale Coupling Framework for Modeling of Large-size Biomass Particle Gasification in Fluidized Beds. Ind. Eng. Chem. Res. **2013**, 52, 11344-11353.

[14] Tinaut, F.V.; Melgar, A.; Perez, J.F.; Horrillo, A. Effect of Biomass Particle Size and Air Superficial Velocity on the Gasification Process in a Downdraft Fixed Bed Gasifier. An Experimental and Modelling Study. Fuel Process. Technol. **2008**, 89, 1076-1089.

[15] Warnecke, R. Gasification of Biomass: Comparison of Fixed Bed and Fluidized Bed Gasifier. Biomass Bioenergy **2000**, 18, 489-497.

[16] Cetin, E.; Moghtaderi, B.; Gupta, R.; Wall, T.F. Influence of Pyrolysis Conditions on the Structure and Gasification Reactivity of Biomass Chars. Fuel **2004**, 83, 2139-2150.

[17] Lv, P.M.; Xiong, Z.H.; Chang, J.; Wu, C.Z.; Chen, Y.; Zhu, J.X. An Experimental Study on Biomass Air–steam Gasification in a Fluidized Bed. Bioresour. Technol. **2004**, 95, 95-101.

[18] Fraga, A.R.; Gaines, A.F.; Kandiyoti, R. Characterization of Biomass Pyrolysis Tars Produced in the Relative Absence of Extraparticle Secondary Reactions. Fuel **1991**, 70, 803-809.

[19] Luo, Z.; Wang, S.; Liao, Y.; Zhou, J.; Gu, Y.; Cen, K. Research on Biomass Fast Pyrolysis for Liquid Fuel. Biomass Bioenergy **2004**, 26, 455-462.

[20] Asadullah, M.; Zhang, S.; Min, Z.; Yimsiri, P.; Li, C.-Z. Importance of Biomass Particle Size in Structural Evolution and Reactivity of Char in Steam Gasification. Ind. Eng. Chem. Res. **2009**, 48, 9858-9863.

[21] Asadullah, M.; Zhang, S.; Li, C.-Z. Evaluation of Structural Features of Chars from Pyrolysis of Biomass of Different Particle Sizes. Fuel Process. Technol. **2010**, 91, 877-881.

[22] Zhang, S.; Min, Z.; Tay, H.L.; Wang, Y.; Dong, L.; Li, C.-Z. Changes in Char Structure during the Gasification of Mallee Wood: Effect of Particle Size and Steam Supply. Energy Fuels **2012**, 26, 193-198.

[23] Sharma, A.; Pareek, V.; Zhang, D. Biomass Pyrolysis–A Review of Modelling, Process Parameters and Catalytic Studies. Renew. Sust. Energ. Rev. **2015**, 50, 1081-1096.

[24] Demirbas, A. Effects of Temperature and Particle Size on Bio-char Yield from Pyrolysis of Agricultural Residues. J. Anal. Appl. Pyrolysis **2004**, 72, 243-248.

[25] Koufopanos, C.A.; Papayannakos, N.; Maschio, G.; Lucchesi, A. Modelling of the Pyrolysis of Biomass Particles. Studies on Kinetics, Thermal and Heat Transfer Effects. Can. J. Chem. Eng. **1991**, 69, 907-915.

[26] Lu, H.; Ip, E.; Scott, J.; Foster, P.; Vickers, M.; Baxter, L.L. Effects of Particle Shape and Size on Devolatilization of Biomass Particle. Fuel **2010**, 89, 1156-1168.

[27] Li, T.; Zhang, L.; Dong, L.; Li, C.-Z. Effects of Gasification Atmosphere and Temperature on Char Structural Evolution during the Gasification of Collie Sub-bituminous Coal. Fuel **2014**, 117, 1190-1195.

[28] Wang, S.; Li, T.; Wu, L.; Zhang, L.; Dong, L.; Hu, X.; Li, C.-Z. Second-order Raman Spectroscopy of Char during Gasification. Fuel Process. Technol. **2015**, 135, 105-111.

[29] Li, X.; Hayashi, J.-I.; Li, C.-Z. FT-Raman Spectroscopic Study of the Evolution of Char Structure during the Pyrolysis of a Victorian Brown Coal. Fuel **2006**, 85, 1700-1707.

[30] Tay, H.-L.; Li, C.-Z. Changes in Char Reactivity and Structure during the Gasification of a Victorian Brown Coal: Comparison between Gasification in O_2 and CO_2. Fuel Process. Technol. **2010**, 91, 800-804.

[31] Tay, H.-L.; Kajitani, S.; Zhang, S.; Li, C.-Z. Effects of Gasifying Agent on the Evolution of Char Structure during the Gasification of Victoria Brown Coal. Fuel **2013**, 103, 22-28.

[32] Sadezky, A.; Muckenhuber, H.; Grothe, H.; Niessner, R.; Poschl, U. Raman Microspectroscopy of Soot and Related Carbonaceous Materials: Spectral Analysis and Structural Information. Carbon **2005**, 43, 1731-1742.

[33] Shimada, T.; Sugai, T.; Fantini, C.; Souza, M.; Cancado, L.G.; Jorio, A. Origin of the 2450 cm^{-1} Raman Bands in HOPG, Single-wall and Double-wall Carbon Nanotubes. Carbon **2005**, 43, 1049-1054.

[34] Zaida, A.; Bar-Ziv, E.; Radovic, L.R.; Lee, Y.-J. Further Development of Raman Microprobe Spectroscopy for Characterization of Char Reactivity. Proc. Combust. Inst. **2007**, 31, 1881-1887.